



Publication Year	2009
Acceptance in OA	2023-02-08T10:45:42Z
Title	Planck-LFI CPV: front end amplifier bias HYM_TUNING
Authors	BATTAGLIA, Paola Maria, Bersanelli, Marco, CUTTAIA, FRANCESCO, Davis, Richard, Wilkinson, Althea, FRAILIS, Marco, Franceschet, Cristian, FRANCESCHI, ENRICO, GALEOTTA, Samuele, GREGORIO, Anna, Leonardi, Rodrigo, Lowe, Stuart, Mandolesi, NAZZARENO, MARIS, Michele, Meinhold, Peter, Mendes, Luis, MENNELLA, ANIELLO, Poutanen, Torsti, SANDRI, MAURA, TAVAGNACCO, Daniele, TERENCE, LUCA, Tomasi, Maurizio, VILLA, Fabrizio, ZACCHEI, Andrea, Zonca, Andrea, DE ROSA, Adriano Giuseppe, MORGANTE, GIANLUCA, Pearson, Dave, VALENZIANO, Luca
Handle	http://hdl.handle.net/20.500.12386/33261
Volume	PL-LFI-PST-RP-068



Planck-LFI CPV: front end amplifier bias HYM_TUNING

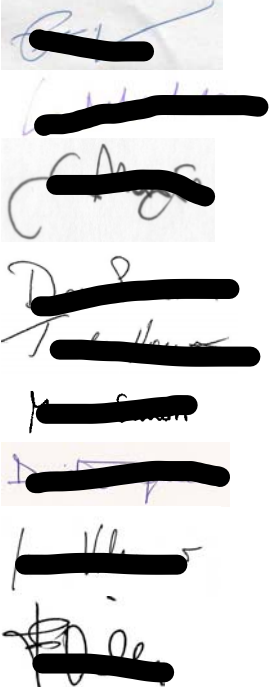

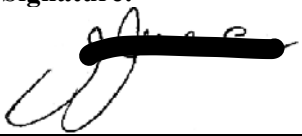
TITLE: (P_PVP_LFI_0105_01, P_PVP_LFI_0105_02, P_PVP_LFI_0105_03,
P_PVP_LFI_0105_04)

DOC. TYPE: Test Report

PROJECT REF.: PL-LFI-PST-RP-068 **PAGE:** I of IV, 11
ISSUE/REV.: 1.0 **DATE:** October 10th, 2009

Prepared by	Signature:	Date: 10 October 2009
Francesco Cuttaia		
Luca Terenzi		
Andrea Zonca		
Paola Battaglia		
Marco Bersanelli		
Richard Davis		
Cristian Franceschet		
Marco Frailis		
Anna Gregorio		
Aniello Mennella		
Maurizio Tomasi		
Althea Wilkinson		
Andrea Zacchei		
A. De Rosa		
Enrico Franceschi		
Samuele Galeotta		
Rodrigo Leonardi		
Stuart Lowe		
Reno Mandolesi		
Michele Maris		
Peter Meinhold		
Luis Mendes		
Gianluca Morgante		
Dave Pearson		
Torsti Poutanen		
Maura Sandri		
Daniele Tavagnacco		
Luca Valenziano		
Fabrizio Villa		



		
<p>Agreed by</p>	<p>C. BUTLER LFI Program Manager</p>	<p>Date: 10 October 2009 Signature: </p>
<p>Approved by</p>	<p>N. MANDOLESI LFI Principal Investigator</p>	<p>Date: 10 October 2009 Signature: </p>



The Planck-LFI calibration team

- Paola Battaglia (SCOS/TQL operator)
- Marco Bersanelli (LFI instrument scientist, test leader)
- Francesco Cuttaia (CPV manager, test leader, data analysis)
- Richard Davis (30/44 GHz data analysis)
- A. De Rosa (SCOS/TQL operator)
- Marco Frailis (Level 1 manager)
- Cristian Franceschet (SCOS/TQL operator)
- Enrico Franceschi (GSE manager)
- Samuele Galeotta (LIFE/PEGASO development)
- Anna Gregorio (Instrument Operation Manager)
- Rodrigo Leonardi (data analysis)
- Stuart Lowe (LIFE/PEGASO development)
- Reno Mandolesi (Principal Investigator)
- Michele Maris (data analysis, LIFE/PEGASO development)
- Peter Meinhold (Test leader, data analysis)
- Luis Mendes (data analysis)
- Aniello Mennella (Calibration Scientist, test leader, data analysis)
- Gianluca Morgante (SCS support to LFI)
- Dave Pearson (SCS support to LFI)
- Torsti Poutanen (data analysis)
- Maura Sandri (Test leader, data analysis)
- Daniele Tavagnacco (SCOS/TQL operator)
- Luca Terenzi (Tests leader, data analysis and LIFE/PEGASO development)
- Maurizio Tomasi (Test leader, data analysis and LIFE/PEGASO development)
- Luca Valenziano (SCOS/TQL operator)
- Fabrizio Villa (Test leader, data analysis)
- Althea Wilkinson (30/44 GHz data analysis)
- Andrea Zacchei (LFI DPC manager)
- Andrea Zonca (SCOS/TQL operator, LIFE/PEGASO development)



DISTRIBUTION LIST

Recipient	Company / Institute	E-mail address	Sent
M. BERSANELLI	UNIMI – Milano	marco.bersanelli@mi.infn.it	Yes
R.C. BUTLER	INAF/IASF – Bologna	butler@iasfbo.inaf.it	Yes
F. CUTTAIA	INAF/IASF – Bologna	cuttaia@iasfbo.inaf.it	Yes
A. GREGORIO	UniTs – Trieste	Anna.gregorio@ts.infn.it	Yes
N. MANDOLESI	INAF/IASF – Bologna	mandolesi@iasfbo.inaf.it	Yes
A. MENNELLA	UNIMI – Milano	aniello.mennella@fisica.unimi.it	Yes
A. ZACCHEI	INAF/OATs – Trieste	zacchei@oats.inaf.it	Yes
ESA Recipients			Yes
TAS-F recipients			Yes
TAS-I recipients			Yes
LFI Core team coordinators		lfi_ctc@iasfbo.inaf.it	Yes
LFI radiometer core team		planck_cta02@fisica.unimi.it	Yes
LFI calibration team			
LFI System PCC	INAF/IASF – Bologna	lfispcc@iasfbo.inaf.it	Yes



TABLE OF CONTENTS

1	ACRONYMS	1
2	APPLICABLE AND REFERENCE DOCUMENTS	2
2.1	APPLICABLE DOCUMENTS	2
2.2	REFERENCE DOCUMENTS	2
3	INTRODUCTION	3
3.1	TEST DESCRIPTION	3
3.2	EXPECTED OUTPUT	5
3.3	ANALYSIS AND HYM MATRIX PRODUCTION	5
3.3.1	<i>Vd Tuning analysis</i>	6
3.3.2	<i>Non linear analysis</i>	6
4	TEST EXECUTION	7
4.1	TEST CONFIGURATION	8
4.2	PASS - FAIL CRITERIA, VERIFICATION MATRIX	9
4.3	PROCEDURE/ TEST SEQUENCE AND ENVIRONMENTAL CONDITIONS	10
4.3.1	<i>Test procedure</i>	10
4.3.2	<i>Temperatures</i>	11
4.3.3	<i>Default bias</i>	13
4.4	RESULTS AND CONCLUSIONS	15
4.4.1	<i>Consistency with Pre Tuning (1st step)</i>	15
4.4.2	<i>Consistency with CSL results</i>	15
4.4.3	<i>Analysis of the Non Linear behaviour</i>	16
4.4.4	<i>Analysis of the signal drift</i>	16
4.5	FINAL BIAS	18
4.6	CONCLUSIONS	24
5	APPENDIX	25
5.1	APPENDIX 1 – 4K TEMPERATURES DURING THE 4 TUNING RUNS	25
5.2	APPENDIX 2– DRAIN VOLTAGE TUNING CURVES	25
5.3	APPENDIX 3 – COMPARISON HYM Vs CSL RESULTS	25
5.4	APPENDIX 4 – 4 TH RUN MAPS WITH PRE-TUNING METHOD	25
5.5	APPENDIX 5 – HYM- MAPS: LINEAR ANALYSIS	25
5.6	APPENDIX 6 –HYM MAPS CORRECTED FOR NON LINEARITY	25
5.7	APPENDIX 7-A –HYM MAPS CORRECTED FOR NON LINEARITY AND BEU THERMAL DRIFT (CUT 3 SIGMA)	25
5.8	APPENDIX 7-B –HYM MAPS CORRECTED FOR NON LINEARITY AND BEU THERMAL DRIFT (CUT 10 SIGMA)	25



1 ACRONYMS

AIV	Assembly, Integration, Verification
ASW	Application Software
BEM	Back End Module
BEU	Back End Unit
CCS	Central Check-out System
CDMU	Central Data Management Unit
CPV	Calibration Performance Verification
CSL	Centre Spatiale de Liège
DAE	Data Acquisition Electronics
DPU	Digital Processing Unit
EGSE	Electrical ground Support Equipment
FEM	Front End Module
I-EGSE	Instrument EGSE
IST	Integrated Satellite Test
OBC	On Board Clock
RAA	Radiometer Array Assembly
REBA	Radiometric Electronic Box Assembly
S/C	Spacecraft
SCOE	Spacecraft Control and Operation System
SCS	Sorption Cooler System
SPU	Signal Processing Unit
SUSW	Start- Up Software
SVM	Service Module
TBC	To Be Checked
TBW	To Be Written
TC	Telecommand
TM	Telemetry
UFT	Unit Functional Test



2 APPLICABLE AND REFERENCE DOCUMENTS

2.1 Applicable Documents

- [AD1] Herschel/Planck Instrument Interface document Part A, SCI-PT-IIDA-04624 Issue 3.3
- [AD2] Herschel/Planck Instrument Interface document Part B, SCI-PT-IIDB-04142 Issue 3.1
- [AD3] Herschel/Planck Instrument Interface document Part B, SCI-PT-IIDB-04142 Issue 3.1, Annex 3, ICD 750800115
- [AD4] Herschel/Planck Instrument Interface document Part A, SCI-PT-IIDA-04624 Issue 3.3 Annex 10
- [AD5] Data analysis and scientific performance of the LFI FM instrument, PL-LFI-PST-AN-006 3.0
- [AD6] Planck-LFI TV-TB test report: executive summary, PL-LFI-PST-RP-040 1.1

2.2 Reference Documents

- [RD1] Planck Instrument Testing at PFM S/C levels, H-P-3-ASP-TN-0676, Issue 1.0
- [RD2] Planck LFI User Manual, PL-LFI-PST-MA-001 Issue 2.1
- [RD3] Data analysis and of LFI switch on and cryogenic functionality test (Ph-5-01-c of TV/TB tests) PL-LFI-PST-RP-036
- [RD4] Change in bias tuning approach during the CPV phase after the CSL test campaign experience PL-LFI-PST-TN-091
- [RD5] Planck-LFI CPV: front end amplifier bias pre-tuning, PL-LFI-PST-RP-067
- [RD6] TUNING OF PLANCK-LFI LNAs IN CPV: REQUIREMENTS SPECIFICATION PL-LFI-PST-SP-017
- [RD7] Testing Plan of the LFI instrument during the Planck Commissioning and CPV phase PL-LFI-PST-PL-013, Issue 4.3 (04-2009)



3 Introduction

This document describes the results from the Hyper-matrix tuning activities.

The Tuning is aimed at finding the optimal bias setting for the LNAs exploring the bias space changing simultaneously the four Vg bias (4-dimensional hypermatrix) powering each radiometer. The hypermatrixes come from the pre-tuning results, drawing for each of the 22 radiometers the bias space around the bias quadruplets expected to produce the best performance (noise temperature and Isolation) . Since Isolation could not intrinsically be measured with the pre-tuning method, Isolation was measured for the first time only at the end of the HYM – TUNING.

In add, for a subset (15 bias quadruplets for each radiometer) of values expected, from pre tuning results , to provide the best performance, also the drain voltage is tuned following a matrix scheme, changing the Vd on both the ACAs of the same radiometer. Hence, for this subset of values, the tuning is performed over a six dimensional hyper space.

3.1 Test description

The test is run 4 times, each at a different temperature of the 4K reference load, advantaging of the 4K cooler cooldown. Output of the test are the Noise Temperature and the Isolation for each of the bias quadruplets applied: it is produced only after the 4th step.

The test consisted in the simultaneous change of Vg1 Vg2 bias powering two paired ACAs (625 Vg11, Vg21, Vg12, Vg22 quadruplets per radiometer) , over several RCAs , grouped following this scheme (minimizing the electric bias cross talk due to the common ground return; see RD4):

GROUP 1: 18-19-22

GROUP 2: 20-21-23

GROUP 3: 24-26-28

GROUP 4: 25-27

At the end of each group, also Vd1 and Vd2 bias were changed for fifteen Vg bias quadruplets.

START CONDITION: All radiometers on, powered with CRYO BIAS (optimal bias from CSL matrix tuning).

Phase switch optimal bias are those coming from the phase switch Tuning (only on 30 GHz and 44 GHz channels: 70 GHz , by default, are set to the maximum DEC values 255 to minimize the phase switch time response)

Tuning is performed group by group.



Group 1: Vg1 (ACA1) , Vg2 (ACA1), Vg1 (ACA2) , Vg2 (ACA2) from RCA 18, 19, 22 are changed in quadruplets; 625 bias quadruplets are exercised. The matrixes in the hyper bias space were drawn basing on the output from the pre-tuning phase. Signal is acquired over 20 seconds for each bias quadruplet.

The same is repeated on radiometer 2 (ACA 3 and 4) over different 625 bias quadruplets.

At the end, Vd tuning is performed (3 VD1 X 3 VD2 combinations are exercised) , following the scheme:

(Vd1,Vd2,Vg11,Vg21,Vg12,Vg22) . The total number of Hexaplets applied is $3 \times 3 \times 15 = 125$

Acquisition time is 20 seconds per each Hexaplet.

Default cryo bias are restored

The same procedure is repeated for the next groups , one by one, until all groups are completed.

The integration time per quadruplet changes with the group under test. It was set to 20 seconds for groups 1 and 2 , to 15 seconds for groups 3, and 4 (grouping 30 GHz and 44 GHz channels that show a shorter signal drift following a bias change). It is instead set to 20 seconds, the same for all the groups, during Vd tuning.

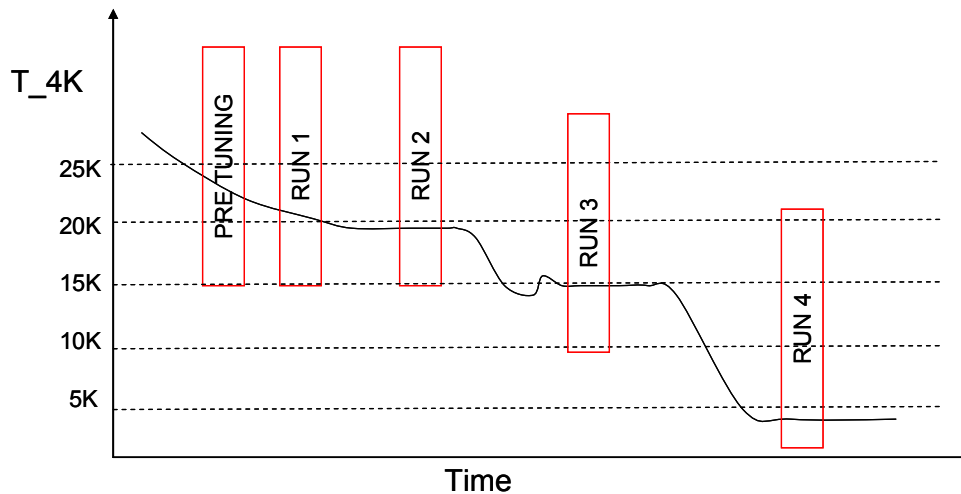


Figure 1 HYM- Tuning Test flow: conceptual description of the 4K cooldown curve with overplotted the tuning phases.



3.2 Expected Output

The test is expected to provide:

- Twenty-two 4 dimensional maps of the noise temperature characterizing each radiometer.
- Twenty-two 4 dimensional maps of the Isolation characterizing each radiometer.
- Twenty-two 4 dimensional maps of the LNAs drain current characterizing each ACA.
- The whole 625 quadruplets bias space is mapped.
- Twenty-two two dimensional plots of Noise Temperature and Isolation versus Vg-Vd Hexaplets : 125 Hexaplets are mapped.
- The final optimal bias table (Vg1, Vg2, Vd) for each ACA producing the best performance.
- The final performance (Noise Temperature and Isolation) table for each radiometer.

The above results are calculated for the 30 and 44 GHz channels both in linear and in non linear regime, applying the non linear 'gain model'.

3.3 Analysis and HYM matrix production.

The analysis is performed using two codes; the first is an IDL code running under LIFE, reading the FITS files, calculating the noise temperature and Isolation and producing for each quadruplet change all the information needed for the analysis (noise Temperature,. Isolation, bias setup, drain currents) . Properties are calculated over just 3 seconds of the whole integration time per bias point, discarding the last 3 seconds and the first 9 or 14 seconds, depending on the channels. This is done in order to minimize the voltage output drift due to the drain current transient when changing the bias. The same time window is selected for the four 4K temperature steps.

This output is ingested into a PYTHON-based code, similar to that used for the Pre tuning analysis, able to display on bi-dimensional maps all the information form the Idl code. Since the bias space is 4-dimensional, the code displays the properties in a concentrated map, where each point collects the average noise temperature or Isolation of the best 20% of the quadruplets sharing the same bias pair. So each point accounts for the average properties of the 4-dim bias space. It is possible to surf inside maps just clicking on each point and cutting the bias space in slices.

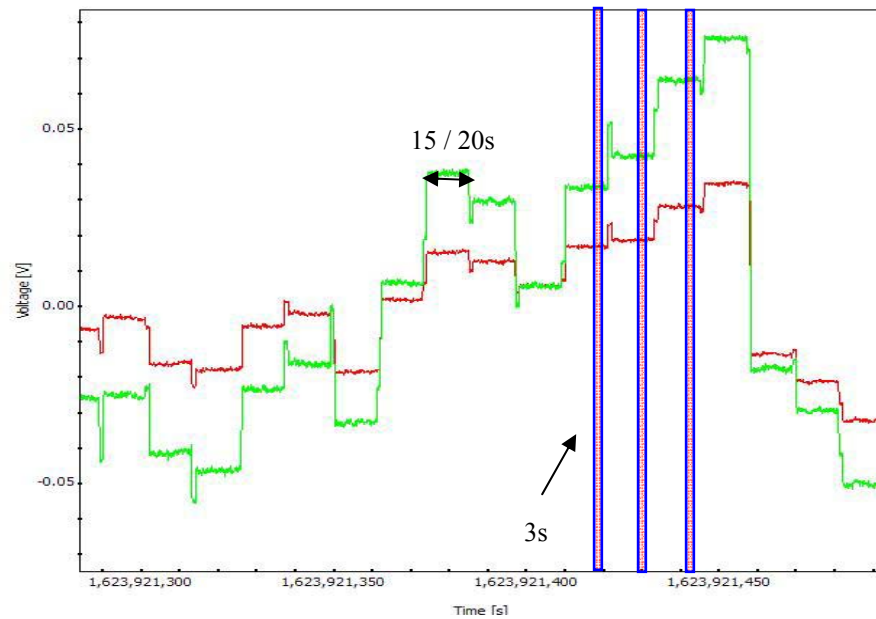


Figure 2 scientific signal from channel RCA 27-00 during HYM Tuning step 1: The total duration of each step (15 s) and the integration time (3 s) are highlighted.

3.3.1 Vd Tuning analysis

Since Vds are tuned only for a limited number of combinations (15 Vg quadruplets coupled with 9 Vd pairs) , results can be displayed on XY plots, where X represents the Vg quadruplet and Y the performance level. Hence 9 curves, corresponding to 9 Vd pairs, are displayed in each plot.

3.3.2 Non linear analysis

Several channels (mainly 44 GHz and 30 GHz) are known from the previous on-ground tests to exhibit non linear response in the BEM stages (amplifiers and diodes), proportional to the input signal from the cold LNAs. This features can be characterized also in-flight by fitting data from the four steps, using a non linear model of the gain, expressly developed for the Tuning (RAA in TAS-Italy and at satellite level in CSL - Liege) . Hence, the IDL code produces both linear and non linear results that, in the same way, can be displayed using the PYTHON code.

Non linearity can also be induced by spurious effects as the BEU thermal drift, inducing changes in the BEM gain. Hence, where evident, these effects should be corrected for.



4 Test Execution

The test started on OD37 (June 19th at) and was fully completed on OD 57 (July 9th).

Despite only four runs (at four different temperatures) were foreseen, some activities were repeated and delayed because of the non nominal thermal conditions of the 4K cooler during the cooldown. In particular, step 4 was repeated due to a REBA crash (putting the LFI in stand by mode). Four runs were performed, following the scheme in the table below.

OD START	OD STOP	TIME START	TIME STOP	STEP
37	38	20090619T19:00:00 UTC	200921T04:12:32 UTC	1
40	41	20090622T22:00:00 UTC	20090624T07:12:32 UTC	2
43	44	20090625T13:30:00 UTC	20090626T22:42:32 UTC	3
55	57	20090707T13:30:00 UTC	20090709T22:42:32 UTC	4 2 nd

Table 1 summary of the time sequence followed for the 4 runs. The 4th run refers to the second execution , since it was repeated twice and for the purpose of the final analysis, the second was considered good.

The thermal conditions are compared with requirements in the table below. Requirements (compare with RD6 and RD7) were set also according to the 4K cooldown prediction based on the HFI thermal model.

T1	T2	SLOPE AVE	SLOPE MAX	T REQ	SLOPE REQ	STEP
19.60	19.11	22mK /h	27 mK /h	23K ± 1K	40mK /h	1
18.61	18.29	20mK /h	30 mK /h	18K ± 1K	15mK /h	2
16.88	16.55	15mK /h	25 mK /h	16K-14K	40mK /h	3
4.75	4.70	< 2mK /h	< 5 mK /h	4.5K + 1K	15mK /h	4

Table 2 Summary of the main thermal properties along the 4 runs for all the power groups. Are represented: T1,T2 (start and stop temperature for each run); thermal slope averaged over the entire duration of the Tuning for each group, for each run;. Maximum slope measured during one hour; 4K temperature required ; 4K maximum fluctuation required.



GROUP	start (s)	stop (s)	T high (K)	T low (K)	Delta T (K)	slope (K/h)
18-19-22 M	1.6241424E+09	1.6241555E+09	19.552	19.472	0.080	-0.022
	1.6244124E+09	1.6244255E+09	18.584	18.527	0.058	-0.016
	1.6246410E+09	1.6246541E+09	16.831	16.783	0.048	-0.013
	1.6258443E+09	1.6258574E+09	4.751	4.751	0.000	0.000
18-19-22 S	1.6241292E+09	1.6241423E+09	19.607	19.540	0.067	-0.018
	1.6243992E+09	1.6244123E+09	18.615	18.561	0.053	-0.015
	1.6246278E+09	1.6246409E+09	16.879	16.824	0.055	-0.015
	1.6258311E+09	1.6258442E+09	4.751	4.751	0.000	0.000
20-21-23 M	1.6241754E+09	1.6241885E+09	19.408	19.343	0.064	-0.018
	1.6244454E+09	1.6244585E+09	18.488	18.431	0.057	-0.016
	1.6246740E+09	1.6246871E+09	16.736	16.689	0.046	-0.013
	1.6258773E+09	1.6258904E+09	4.751	4.751	0.000	0.000
20-21-23 S	1.6241622E+09	1.6241754E+09	19.461	19.392	0.069	-0.019
	1.6244322E+09	1.6244454E+09	18.522	18.463	0.059	-0.016
	1.6246608E+09	1.6246740E+09	16.779	16.736	0.043	-0.012
	1.6258641E+09	1.6258773E+09	4.751	4.751	0.000	0.000
24-26-28 M	1.6241953E+09	1.6242053E+09	19.322	19.273	0.048	-0.017
	1.6244653E+09	1.6244753E+09	18.431	18.388	0.043	-0.016
	1.6246939E+09	1.6247039E+09	16.686	16.645	0.041	-0.015
	1.6258972E+09	1.6259072E+09	4.709	4.708	0.001	0.000
24-26-28 S	1.6241953E+09	1.6242053E+09	19.322	19.273	0.048	-0.017
	1.6244653E+09	1.6244753E+09	18.431	18.388	0.043	-0.016
	1.6246939E+09	1.6247039E+09	16.686	16.645	0.041	-0.015
	1.6258972E+09	1.6259072E+09	4.709	4.708	0.001	0.000
25-27 M	1.6242220E+09	1.6242320E+09	19.210	19.161	0.050	-0.018
	1.6244920E+09	1.6245020E+09	18.362	18.318	0.044	-0.016
	1.6247206E+09	1.6247306E+09	16.611	16.580	0.031	-0.011
	1.6257556E+09	1.6257656E+09	4.709	4.708	0.001	-0.001
25-27 S	1.6242321E+09	1.6242421E+09	19.172	19.117	0.055	-0.020
	1.6245021E+09	1.6245121E+09	18.348	18.293	0.054	-0.020
	1.6247307E+09	1.6247407E+09	16.584	16.556	0.027	-0.010
	1.6257657E+09	1.6257757E+09	4.709	4.706	0.003	-0.001

Table 3 Test execution: start and stop time for each channel and for each run are displayed together with thermal conditions (4 K reference load temperature and average thermal drift per hour)

4.1 Test configuration

The test configuration is the following:

SCOS 2 K HPPCCS Version 2.0.787
LFI Gateway Version V0R9P1
TQL 3.1.2
LIFE Machine version OM 3.00

LFI Personnel involved during the test is:



LFI Instrument Operation Manager	Anna Gregorio (UniTs anna.gregorio@ts.infn.it)
LFI Calibration Scientist	Aniello Mennella (UniMi aniello.mennella@fisica.unimi.it)
LFI CPV Manager	Francesco Cuttaia (IASF-BO cuttaia@iasfbo.inaf.it)
Test leader	Francesco Cuttaia, Aniello Mennella, Luca Terenzi
LFI IOT	Anna Gregorio, Francesco Cuttaia, , Richard Davis, Marco Frailis, Samuele Galeotta, Aniello Mennella, Luca Terenzi, Maurizio Tomasi, Daniele Tavagnacco, Althea Wilkinson, Andrea Zacchei, Andrea Zonca
Industry support	Paola Battaglia

4.2 Pass - fail criteria, verification matrix

Verification matrix RUN 1					
Check	Passed?			Recovered?	
	Yes	No	Notes	Yes	No
No unexpected event Packets	Yes				
TC procedure	Yes				
Every ACA is responding to Biases stimulus as expected	Yes				
No unexpected features	Yes				
Temperature requirement met		No	4K stage temperature is below what expected, around 19.5 K, but cooldown can not be stopped or slow down. This is acceptable	Yes	
Data saved and stored at DPC	Yes				

Verification matrix RUN 2					
Check	Passed?			Recovered?	
	Yes	No	Notes	Yes	No
No unexpected event Packets	Yes				
TC procedure	Yes				
Every ACA is responding to Biases stimulus as expected	Yes				
No unexpected features	Yes				
Temperature requirement met	Yes	No	4K stage temperature is as expected, around 18.6 K 4K fluctuations higher than req.	Yes	
Data saved and stored at DPC	Yes				



Verification matrix RUN 3					
Check	Passed?			Recovered?	
	Yes	No	Notes	Yes	No
No unexpected event Packets	Yes				
TC procedure	Yes				
Every ACA is responding to Biases stimulus as expected	Yes				
No unexpected features	Yes				
Temperature requirement met		No	4K stage temperature is slightly above what expected, around 16.7 K, but it was already agreed that this is acceptable	Yes	
Data saved and stored at DPC	Yes				

Verification matrix RUN 4					
Check	Passed?			Recovered?	
	Yes	No	Notes	Yes	No
No unexpected event Packets	Yes				
TC procedure	Yes				
Every ACA is responding to Biases stimulus as expected	Yes				
No unexpected features		no	The LFI went into an expected mode (REBA crash) due to the time verification TC. See AR P_SC-25. The test has been repeated.	yes	
Temperature requirement met		no	4K fluctuations above the requirements, some blocks have been repeated	yes	
Correct biases Produced, Applied and Checked	Yes				
Data saved and stored at DPC	Yes				

Despite of the red boxes showing that two requirements have not been met (4K temperature requirement and thermal stability), results are however considered accurate for the purpose of the test: this is why the field ‘recovered’ is flagged with Yes. Instead, after the REBA crash during the first execution of the 4th run, the test was repeated and hence results are considered recovered at all.

4.3 Procedure/ Test sequence and environmental conditions

4.3.1 Test procedure

The test sequence, repeated the same for the four runs, is summarized here below. Given the large numbers of Tcs applied, the entire procedure and the values applied were checked automatically by means of an IDL script comparing data with the nominal procedure / bias. This check confirmed that the procedure run successfully.



Step	Description	START REF.	DURATION	RCA
10	ACA Hyper Matrix Tuning (UM § 13.1.2.7)			
10.1	Perform Matrix Tuning Vg1,Vg2	0:00:00	7:19:39	18,19,22
10.2	RCA 18,19,22	7:19:39	0:00:00	18,19,22
10.3	Perform Matrix Tuning Vg1,Vg2,Vd	7:19:39	1:50:07	18,19,22
10.4	RCA 18,19,22	9:09:46	0:00:00	18,19,22
10.5	Perform Matrix Tuning Vg1,Vg2	9:09:46	7:19:39	20,21,23
10.6	RCA 20,21,23	16:29:25	0:00:00	20,21,23
10.7	Perform Matrix Tuning Vg1,Vg2,Vd	16:29:25	1:50:07	20,21,23
10.8	RCA 20,21,23	18:19:32	0:00:00	20,21,23
10.9	Perform Matrix Tuning Vg1,Vg2	18:19:32	5:35:39	24,26,28
10.10	RCA 24,26,28	23:55:11	0:00:00	24,26,28
10.11	Perform Matrix Tuning Vg1,Vg2,Vd	23:55:11	1:50:07	24,26,28
10.12	RCA 24,26,28	25:45:18	0:00:00	24,26,28
10.13	Perform Matrix Tuning	25:45:18	5:35:39	25,27
10.14	RCA 25,27	31:20:57	0:00:00	25,27
10.15	Perform Matrix Tuning Vg1,Vg2,Vd	31:20:57	1:50:07	25,27
10.16	RCA25,27	33:11:04	0:00:00	25,27
10.17	End of tests		33:11:04	

Table 4 HYM Tuning schematic procedure.

4.3.2 Temperatures

The sensors used to track the relevant temperatures and to perform the data analysis are:

4K temperature

For runs 1,2,3 the sensor:

HD028260 (SCOS name)

was used for all the loads. This is because it was the only having calibration curves in the thermal range explored. The sensor is put very close to the 4K cold end. Data are sampled at 1Hz.

For the 4th run different sensors were used for the 30/44 GHz loads and for the 70 GHz loads. This is why more sensitive sensors were available below 7K , located closer to the loads.

HFI Ther_PID4N1 was used to characterize the 70 GHz 4K reference loads

HFI Ther_PID_4KL1 was used to characterize the 30 and 44 GHz 4K Reference loads.

These sensors were provided by HFI sampled at 180 Hz and were re-sampled at 2 Hz.

The entire test took a long time to be completed: this is due to the initial schedule, foreseeing to perform the forth run after 4 days from the completion of the 4K cooldown (to allow HFI activities in the meanwhile) and due to some thermal instabilities occurred on the 4K stage,



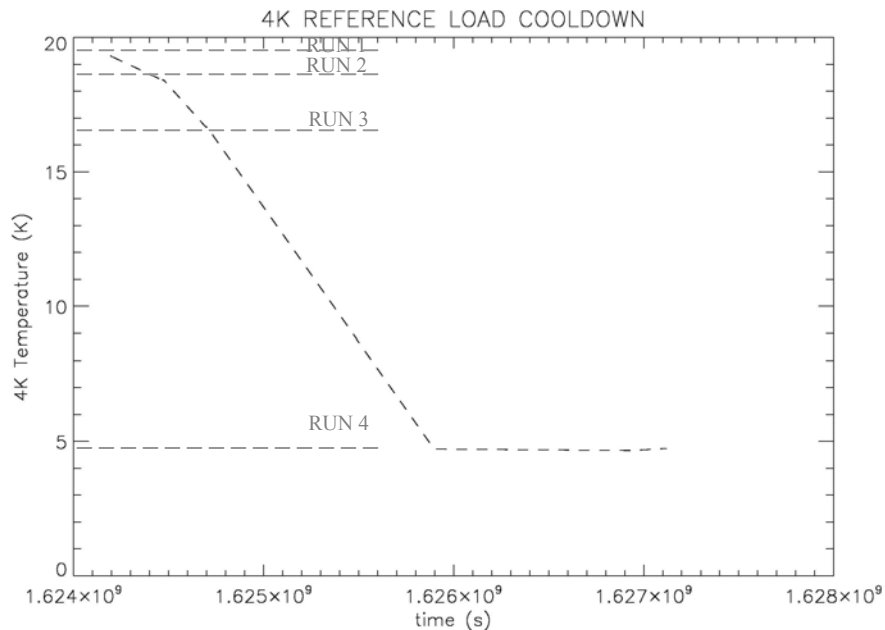
requiring to repeat twice the fourth step. Moreover, a REBA crash occurred on day XXX required to repeat the 4th run twice.

BEU and FEU sensors:

During the 20 days required to complete the test, other sensitive quantities, apart from the 4K temperature, changed. This is especially the case of the BEM temperatures: we tried to correct for these changes in the data analysis.

SENSOR	RUN 1	RUN 2	RUN 3	RUN 4-a	RUN 4-b
RBEM 1	17.73	17.75	18.09	18.07	17.96
LBEM 1	14.97	15	15.34	15.3	15.18
LFEM 1	19.32	19.4	19.71	19.68	19.56
RFEM 1	19.47	19.5	19.83	19.82	19.72
F 28	19.585	19.587	19.583	19.59	19.58
F26	20.265	20.267	20.26	20.26	20.26
F25	20.405	20.408	20.399	20.405	20.399
CR	19.744	19.746	19.741	19.747	19.743
CL	20.242	20.25	20.162	20.251	20.244

Table 5 Temperatures of interest for the HYM-Tuning during the 5 runs (two runs repeated at 4 K due to the REBA crash and 4K instabilities)



Plot 1 4K reference load cooldown profile during the Tuning; The total duration was about 20 days The horizontal dashed lines represents the 4K temperature when each run started..

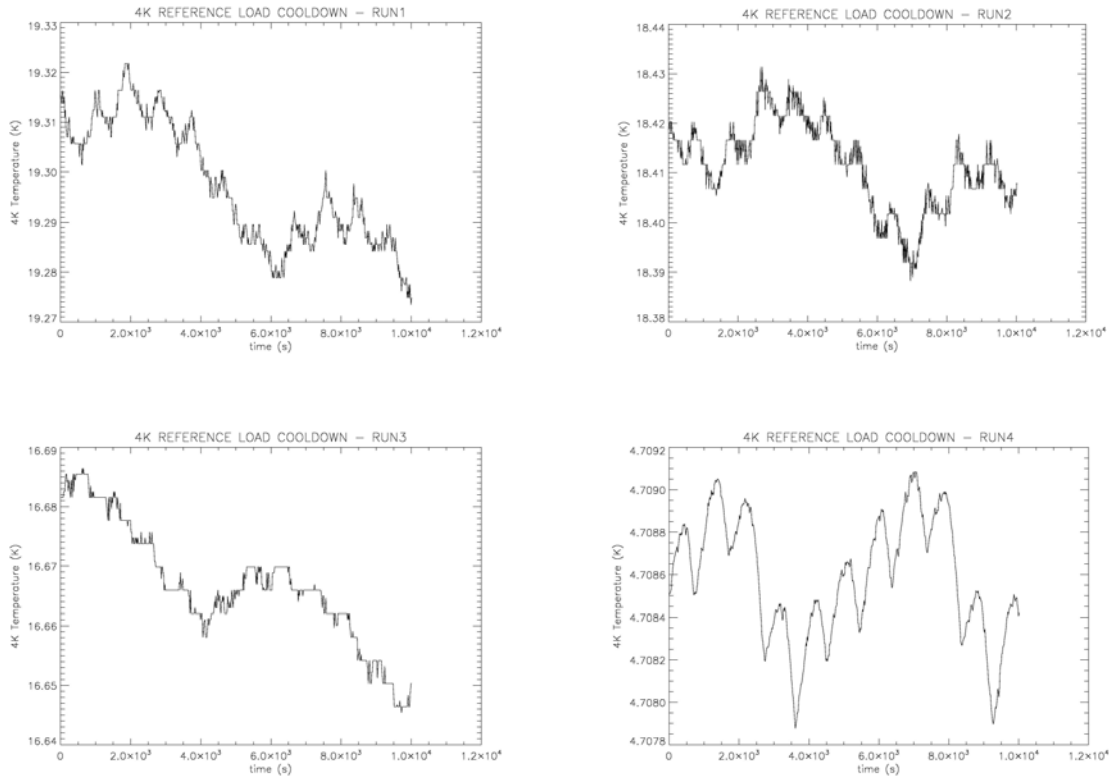


Figure 3 Example of the 4K temperature fluctuations during Tuning of radiometers belonging to the first power group along the 4 runs. Full results are reported in Appendix 1

4.3.3 Default bias

The LNAs bias configuration set as default (on channels not under test) is the same used for the Pre-Tuning.

LNAs Bias matrix are instead the outcome of the Pre-Tuning analysis.

The default configuration is reported in Figure 4



					vg1		vg2		vd		I1		I2		G		O	
CH27	00	00	M1	LP001320	240	F0	108	6C	156	9C	178	B2	180	B4				
CH27	01	01	M2	LP002320	244	F4	90	5A	157	9D	144	90	214	D6				
CH27	02	10	S1	LP003320	237	ED	102	66	157	9D	138	8A	192	C0				
CH27	03	11	S2	LP004320	246	F6	114	72	156	9C	128	80	200	C8				
CH24	04	00	M2	LP005320	227	E3	213	D5	183	B7	91	5B	255	FF				
CH24	05	01	M1	LP006320	219	DB	217	D9	183	B7	128	80	250	FA				
CH24	06	10	S2	LP007320	225	E1	213	D5	152	98	86	56	215	D7				
CH24	07	11	S1	LP008320	219	DB	219	DB	157	9D	84	54	235	EB				
CH21	08	00	S2	LP009320	216	D8	223	DF	132	84	255	FF	255	FF				
CH21	09	01	S1	LP010320	181	B5	197	C5	136	88	255	FF	255	FF				
CH21	0A	10	M1	LP011320	198	C6	207	CF	141	8D	255	FF	255	FF				
CH21	0B	11	M2	LP012320	196	C4	197	C5	136	88	255	FF	255	FF				
CH22	0C	00	S2	LP013320	206	CE	204	CC	130	82	255	FF	255	FF				
CH22	0D	01	S1	LP014320	204	CC	189	BD	128	80	255	FF	255	FF				
CH22	0E	10	M1	LP015320	203	CB	194	C2	125	7D	255	FF	255	FF				
CH22	0F	11	M2	LP016320	178	B2	176	B0	130	82	255	FF	255	FF				
CH23	10	00	S2	LP017320	190	BE	208	D0	122	7A	255	FF	255	FF				
CH23	11	01	S1	LP018320	181	B5	211	D3	118	76	255	FF	255	FF				
CH23	12	10	M1	LP019320	207	CF	192	C0	120	78	255	FF	255	FF				
CH23	13	11	M2	LP020320	210	D2	195	C3	119	77	255	FF	255	FF				
CH25	14	00	M1	LP021320	227	E3	212	D4	184	B8	174	AE	235	EB				
CH25	15	01	M2	LP022320	219	DB	212	D4	185	B9	89	59	250	FA				
CH25	16	10	S1	LP023320	224	E0	216	D8	167	A7	93	5D	255	FF				
CH25	17	11	S2	LP024320	223	DF	212	D4	166	A6	119	77	225	E1				
CH28	18	00	M1	LP025320	243	F3	101	65	157	9D	132	84	162	A2				
CH28	19	01	M2	LP026320	240	F0	112	70	156	9C	117	75	188	BC				
CH28	1A	10	S1	LP027320	240	F0	84	54	157	9D	111	6F	168	A8				
CH28	1B	11	S2	LP028320	245	F5	121	79	158	9E	99	63	173	AD				
CH20	1C	00	S2	LP029320	188	BC	201	C9	127	7F	255	FF	255	FF				
CH20	1D	01	S1	LP030320	199	C7	221	DD	132	84	255	FF	255	FF				
CH20	1E	10	M1	LP031320	209	D1	219	DB	121	79	255	FF	255	FF				
CH20	1F	11	M2	LP032320	215	D7	221	DD	127	7F	255	FF	255	FF				
CH19	20	00	S2	LP033320	204	CC	216	D8	125	7D	255	FF	255	FF				
CH19	21	01	S1	LP034320	215	D7	209	D1	120	78	255	FF	255	FF				
CH19	22	10	M1	LP035320	213	D5	206	CE	124	7C	255	FF	255	FF				
CH19	23	11	M2	LP036320	211	D3	208	D0	126	7E	255	FF	255	FF				
CH18	24	00	S2	LP037320	208	D0	205	CD	114	72	255	FF	255	FF				
CH18	25	01	S1	LP038320	192	C0	197	C5	138	8A	255	FF	255	FF				
CH18	26	10	M1	LP039320	190	BE	194	C2	126	7E	255	FF	255	FF				
CH18	27	11	M2	LP040320	198	C6	201	C9	125	7D	255	FF	255	FF				
CH26	28	00	M2	LP041320	226	E2	217	D9	170	AA	153	99	210	D2				
CH26	29	01	M1	LP042320	232	E8	209	D1	169	A9	98	62	245	F5				
CH26	2A	10	S2	LP043320	232	E8	217	D9	169	A9	93	5D	230	E6				
CH26	2B	11	S1	LP044320	228	E4	226	E2	172	AC	135	87	230	E6				
CH27	00	00	M1	LP001320											0	0	21	15
CH27	01	01	M2	LP002320											0	0	0	0
CH27	02	10	S1	LP003320											0	0	51	33
CH27	03	11	S2	LP004320											0	0	50	32
CH24	04	00	M2	LP005320											0	0	255	FF
CH24	05	01	M1	LP006320											0	0	255	FF
CH24	06	10	S2	LP007320											0	0	255	FF
CH24	07	11	S1	LP008320											0	0	255	FF
CH21	08	00	S2	LP009320											0	0	194	C2
CH21	09	01	S1	LP010320											0	0	204	CC
CH21	0A	10	M1	LP011320											0	0	180	B4
CH21	0B	11	M2	LP012320											0	0	180	B4
CH22	0C	00	S2	LP013320											0	0	255	FF
CH22	0D	01	S1	LP014320											0	0	255	FF
CH22	0E	10	M1	LP015320											0	0	255	FF
CH22	0F	11	M2	LP016320											0	0	255	FF
CH23	10	00	S2	LP017320											0	0	100	64
CH23	11	01	S1	LP018320											0	0	100	64
CH23	12	10	M1	LP019320											0	0	180	B4
CH23	13	11	M2	LP020320											0	0	180	B4
CH25	14	00	M1	LP021320											0	0	255	FF
CH25	15	01	M2	LP022320											0	0	255	FF
CH25	16	10	S1	LP023320											0	0	255	FF
CH25	17	11	S2	LP024320											0	0	255	FF
CH28	18	00	M1	LP025320											0	0	60	3C
CH28	19	01	M2	LP026320											0	0	41	29
CH28	1A	10	S1	LP027320											0	0	60	3C
CH28	1B	11	S2	LP028320											0	0	143	8F
CH20	1C	00	S2	LP029320											0	0	128	80
CH20	1D	01	S1	LP030320											0	0	128	80
CH20	1E	10	M1	LP031320											0	0	128	80
CH20	1F	11	M2	LP032320											0	0	128	80
CH19	20	00	S2	LP033320											0	0	214	D6
CH19	21	01	S1	LP034320											0	0	204	CC
CH19	22	10	M1	LP035320											0	0	220	DC
CH19	23	11	M2	LP036320											0	0	224	E0
CH18	24	00	S2	LP037320											0	0	0	0
CH18	25	01	S1	LP038320											0	0	0	0
CH18	26	10	M1	LP039320											0	0	128	80
CH18	27	11	M2	LP040320											0	0	128	80
CH26	28	00	M2	LP041320											0	0	255	FF
CH26	29	01	M1	LP042320											0	0	255	FF
CH26	2A	10	S2	LP043320											0	0	255	FF
CH26	2B	11	S1	LP044320											0	0	255	FF

Figure 4 default CRYO bias table applied for the test



4.4 Results and Conclusions

The procedure was successfully run without any problem. All the bias effectively applied were verified to be compliant with the input matrixes, using an IDL code extracting bias from the test data and comparing with the test procedure.

Results from the HYM Tuning maps were consistent with those from the Pre-Tuning.

Not always the best performance bias quadruplet was chosen as the optimal bias point: in fact, optimal bias were chosen case by case, crossing the information coming from Noise Temperature, Isolation, drain current. In some cases it was preferred to pay something in terms of noise temperature in order to improve the radiometer balancing (making the drain currents flowing on two coupled ACAs the closer the possible) .

Vd tuning was also considered in the choice of the final exa-plets: however Vd was changed w.r.t. default values only in the case that a clear improvement was evident and that the nine Vd curves per radiometer were clearly separated for all the Vg quadruplets applied.

Also the non linear model (Gain model) was applied to 30 and 44 GHz channels to check for possible different indications in the choice of the region containing minima. Full results in appendix 5.6

At the end, a model corrected for the BEM thermal drift was applied and cross-checked with the previous results. Full results in appendix 5.7

The final optimal bias table was produced (Table 9).

4.4.1 Consistency with Pre Tuning (1st step)

Comparison with Pre Tuning results (maps / table) are showed a very good capability of the pre-tuning method to provide a guess of the overall Noise Temperature. For a complete comparison see RD 5.

4.4.2 Consistency with CSL results

Comparison with CSL results (maps + table) is reported in Appendix 5.3: Noise Temperature was calculated for the bias quadruplets common to CSL and CPV tuning. The number of samples depends on the channel, and hence also the resolution of each map. Due to the point selection criteria adopted to build CPV maps following the Pre Tuning, in some cases only a few quadruplets are available, making the comparison very rough.

In all the other cases, results show a discrete agreement with those from from CSL Tuning, confirming the validity of the method followed and showing that the LFI radiometers did not change their overall behaviour.



4.4.3 Analysis of the Non Linear behaviour

The Gain non linear model was applied to the detectors output to investigate the possible impact of non linearity on the choices of the final bias table. This analysis was not straight because of all the other effects affecting the radiometers output and possibly masking or mimicking non linear effects.

One limiting factor is represented without doubt by the knowledge of the reference loads temperature, only rough since , above 7 K , only one HFI thermometer (as in CSL) was calibrated ; moreover this thermometer is located near to the 4K cold-end , hence far from the reference loads.

Other limiting factors were represented by the BEU thermal fluctuations, producing a spurious gain variation in the back end amplifiers.

Results from the Non linear Gain model, applied without corrections, are displayed in Appendix 5.6

4.4.4 Analysis of the signal drift

Tuning Maps were also calculated correcting the output voltage for the thermal drift of the BEU during the four steps. The correction terms were at 1st order calculated imposing the coincidence of the sky signal during the four runs of the Tuning (hence supposing also perfect isolation between coupled ACAs): variations are in agreement with the known behaviour of the back end amplifiers . This correction was applied to correct the non linear model.

A non negligible change in the BEU temperature was measured after the REBA crash , because the LFI went into stand-by mode and the power groups were switched off. The switch off induced the cooling down of the back end, due to the missing power dissipation . Differences measured by the BEM sensors before and after the crash are displayed in the table below

	04-07-2009	05-07-2009	DELTA
LBEM1	15.38	14.23	-1.15
LBEM2	17.88	16.72	-1.16
LFEM1	19.76	18.62	-1.14
LFEM2	15.37	14.28	-1.09
LDAQ	16.85	15.64	-1.21
RBEM1	18.17	16.98	-1.19
RBEM2	15.6	14.4	-1.2
LFEM1	19.9	18.76	-1.14
LFEM2	16.08	14.9	-1.18
RDAQ	17.17	15.93	-1.24

Table 6 Temperature comparison at BEU level before and after REBA crash.

Complete Results are displayed in Appendix 5.7.

This analysis shows that the optimal bias coming from the linear model produce still very good results when the non linear model, corrected for the back end thermal fluctuation , is applied.



NOISE TEMPERATURE COMPARISON FOR 30 GHz - 44 GHz

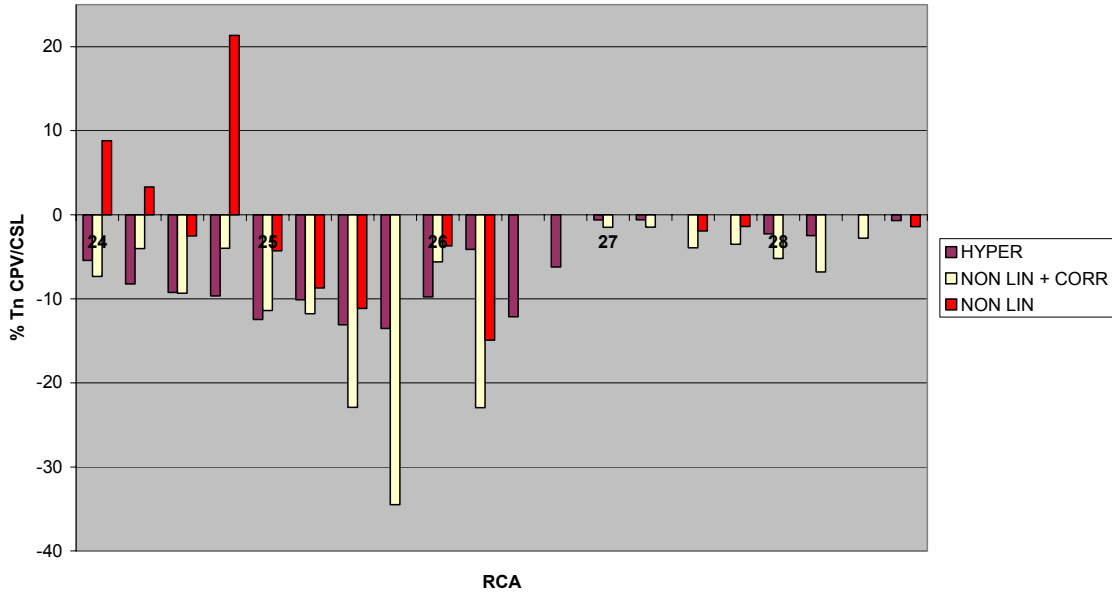
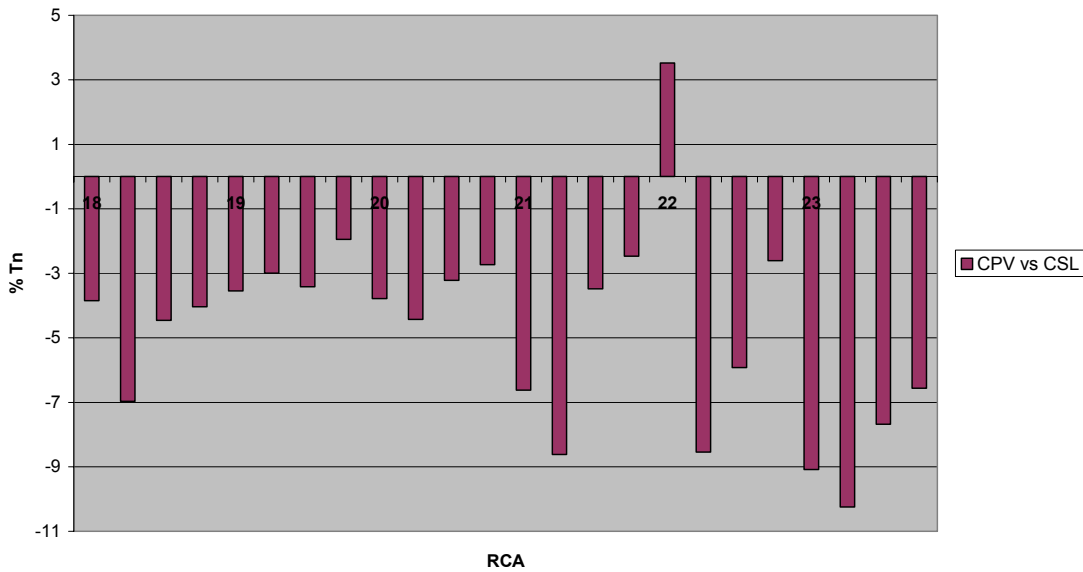


Table 7 Noise Temperature comparison at 44 GHz between CPV and CSL bias in case of linear response (HYPER), Non linear response (NON LIN, the gain model is applied), Non linear response corrected for the BEU thermal drift (NON LIN + CORR); The percent variation is displayed on Y axis.

Noise Temperature Comparison for 70 GHz (Linear case)



Plot 2 Noise Temperature comparison at 70 GHz between CPV and CSL optimal bias using a linear model of the radiometer. The percent variation is displayed on Y axis.



	CPV OPT		GMODEL		G. M. + CORR (cut 10)		CPV	G.M + C	G.M
24 "M2"	227	204	230	211	227	204	-5.4	8.8	-7.3
24 "M1"	219	204	228	208	215	219	-8.2	3.3	-4.0
24 "S2"	225	208	219	213	220	218	-9.2	-2.5	-9.3
24 "S1"	218	207	219	219	210	223	-9.7	21.3	-4.0
25 "M1"	231	203	208	202	237	203	-12.5	-4.3	-11.4
25 "M2"	218	200	222	223	218	200	-10.1	-8.7	-11.8
25 "S1"	231	196	231	191	231	191	-13.1	-11.1	-22.9
25 "S2"	223	199	238	193	232	194	-13.5	0.0	-34.5
26 "M2"	226	200	248	207	232	209	-9.8	-3.7	-5.6
26 "M1"	247	203	238	195	233	207	-4.1	-14.9	-23.0
26 "S2"	240	197	225	201	225	201	-12.1	N.A	N.A
26 "S1"	227	194	231	200	231	200	-6.2	N.A	N.A
27 "M1"	242	97	243	109	240	108	-0.6	N.A	-1.5
27 "M2"	255	96	244	70	253	77	-0.6	N.A	-1.5
27 "S1"	235	86	243	98	238	86	0.0	-1.9	-3.9
27 "S2"	248	113	246	94	255	106	0.0	-1.4	-3.5
28 "M1"	243	101	240	101	240	101	-2.3	0.0	-5.2
28 "M2"	240	112	246	152	237	156	-2.5	0.0	-6.8
28 "S1"	235	81	235	88	234	104	0.0	0.0	-2.8
28 "S2"	249	90	248	121	254	116	-0.7	-1.4	-4.3

Table 8 Comparison between CPV Vg Optimal bias and bias producing the lowest Noise Temperature in the case that a Gain model correction or a gain model + BEM drift correction (sky signal fluctuations considered negligible below 10 sigma) . Performance are compared for the three cases with those coming from CSL bias, measured in the same tests (In this way, possible variations due to the different setup and methods between CSL and CPV are dropped). Results are given in percent of the relative variation w.r.t. to performance measured for the CSL bias quadruplets..

4.5 FINAL BIAS

The choice of the final optimal bias was an outcome of the trade off between performance and other features. A particular care was taken to:

Avoid Noise Temperature minima not belonging to bias regions with showing good performance over a wide bias space (hence, singularities have been avoided, despite of their optimal performance). This was done to prevent the radiometer from possible bias shifts moving it abruptly from good to bad performance.

Combine good Isolation with balancing of drain currents over two coupled ACAs.

Choose a drain voltage different from nominal only in the case that:

- The bias quadruplet tested with that particular Vd pair has a counterpart to be compared with in the 4 runs.
- an evident (> 0.5 K) improvement is shown
- Vd curves show a simple shape in a wise that the improvement is easy to be recognized.



- The bias quadruplet associated with that particular Vd pair provides still quite balanced drain currents in the two paired ACAs.

For each channel, in the case the chosen value does not coincide with the optimal value provided by the Tuning code, the explanation of the reason is given.

The final optimal bias are reported in Table 9., compared to CSL bias.

CSL									CPV							
"FH"	"CH."	"Vg1"	"Vg2"	"Vd"	'Id [mA]'	Tn	Iso		"Vg1"	"Vg2"	"Vd"	'Id [mA]'	Tn	Iso	Tn%	ISO %
18	"S2"	208	205	114	21.5	26.5	N.A.		216	182	114	18.5	25.5	0.033	-3.85	N.A.
18	"S1"	192	197	138	19.8	29.7	N.A.		155	215	138	16.2	27.7	0.037	-6.97	N.A.
18	"M1"	190	194	126	13.5	27.5	N.A.		195	189	126	13.2	26.3	0.032	-4.46	N.A.
18	"M2"	198	201	125	14.4	27.8	N.A.		198	201	125	14.51	26.7	0.026	-4.04	N.A.
19	"S2"	204	216	125	17	28.7	0.025		207	222	125	17.97	27.7	0.026	-3.55	3.9
19	"S1"	215	209	120	17.8	30.5	0.028		202	226	120	18.19	29.6	0.029	-3.00	3.5
19	"M1"	213	206	124	18.1	26.8	N.A.		205	221	124	20.19	25.9	0.049	-3.42	N.A.
19	"M2"	211	208	126	19.8	25.9	N.A.		196	216	126	19.63	25.4	0.034	-1.95	N.A.
20	"S2"	188	201	127	18.5	32.3	0.027		169	215	127	16.99	31.1	0.034	-3.79	23.0
20	"S1"	199	221	132	18.7	32.3	0.027		179	230	132	17.62	30.9	0.031	-4.43	13.8
20	"M1"	209	219	121	20.5	28.4	0.037		191	244	121	21.38	27.5	0.031	-3.22	-17.6
20	"M2"	215	221	127	20.6	29.7	0.0004		209	231	127	21.3	28.9	-0.002	-2.73	300.0
21	"S2"	216	223	132	20.3	31.2	0.16		205	243	132	22.18	29.2	0.028	-6.62	-140.4
21	"S1"	181	197	136	16.5	33.9	0.174		170	221	136	19.24	31.1	0.015	-8.62	-168.3
21	"M1"	198	207	141	18.5	23.4	0.02		192	231	147	21.5	22.6	0.015	-3.48	-28.6
21	"M2"	196	197	136	19.6	24.6	0.027		191	224	136	23.9	24.0	0.028	-2.47	3.6
22	"S2"	206	204	130	15.2	27.9	0.037		193	231	130	19.25	28.9	0.029	3.52	-24.2
22	"S1"	204	189	128	16.6	29.3	0.039		210	221	128	21.41	26.9	0.028	-8.54	-32.8
22	"M1"	203	194	125	14.2	27.9	-0.006		208	218	130	18.87	26.3	-0.006	-5.92	0.0
22	"M2"	178	176	130	14.9	27.7	0.004		188	188	135	18.53	27.0	0.003	-2.60	-28.6
23	"S2"	190	208	122	15	32	0.012		198	213	127	17.74	29.2	0.029	-9.08	82.9
23	"S1"	181	211	118	20.7	31.4	0.009		180	222	123	21.77	28.3	0.021	-10.24	80.0
23	"M1"	207	192	120	14.9	31.1	0.023		211	206	120	17.04	28.8	0.016	-7.68	-35.9
23	"M2"	210	195	119	14.5	29.9	0.027		190	228	119	17.25	28.0	0.015	-6.56	-57.1
24	"M2"	227	213	183	10	20.8	0.007		227	204	183	7.24	19.7	0.006	-5.43	-15.4
24	"M1"	219	217	183	11.3	22.8	0.015		219	204	183	7.36	21.0	0.017	-8.22	12.5
24	"S2"	225	213	152	9.9	23.8	0.028		225	208	152	7.8	21.7	0.026	-9.23	-7.4
24	"S1"	219	219	157	12.8	22.8	0.029		218	207	157	8.3	20.7	0.029	-9.66	0.0
25	"M1"	227	212	184	9.3	24.7	0.016		231	203	177	6.29	21.8	0.015	-12.47	-6.5
25	"M2"	219	212	185	9.9	23.9	0.016		218	200	178	6.29	21.6	0.015	-10.11	-6.5
25	"S1"	224	216	167	11.1	22.8	0.001		231	196	167	6.07	20.0	-0.002	-13.08	600.0
25	"S2"	223	212	166	9.5	22.9	0.003		223	199	166	5.96	20.0	0.004	-13.52	28.6
26	"M2"	226	217	170	11.7	29	0.047		226	200	170	8.22	26.3	0.024	-9.76	-64.8
26	"M1"	232	209	169	8.1	24.8	0.042		247	203	169	7.86	23.8	0.032	-4.12	-27.0
26	"S2"	232	217	169	10.4	24.5	0.007		240	197	169	6.07	21.7	0.005	-12.12	-33.3
26	"S1"	228	226	172	13.4	21.6	0.017		227	194	172	6.29	20.3	0.018	-6.21	5.7
27	"M1"	240	108	156	8.1	16.7	0.009		242	97	156	7.98	16.6	0.008	-0.60	-11.8
27	"M2"	244	90	157	7.2	17	0.008		255	96	157	7.57	16.9	0.005	-0.59	-46.2
27	"S1"	237	102	157	8.5	19.2	0.003		235	86	157	8.26	19.2	0.004	0.00	28.6
27	"S2"	246	114	156	8	17.2	0.005		248	113	156	8.04	17.2	0.006	0.00	18.2
28	"M1"	243	101	157	9.6	16.1	0.025		243	101	150	8.99	15.7	0.02	-2.26	-22.2
28	"M2"	240	112	156	9.2	16.4	0.034		240	112	163	9.77	16.0	0.026	-2.47	-26.7
28	"S1"	240	84	157	9.1	16.1	0.043		235	81	157	8.81	16.1	0.043	0.00	0.0
28	"S2"	245	121	158	10.4	15	0.045		249	90	158	9.36	14.9	0.043	-0.67	-4.5

Table 9 optimal bias from HYM tuning. Noise temperature and Isolation are displayed. Red numbers indicate that the field was changed w.r.t. the CSL bias.

It is important to notice that, once the final bias table was applied simultaneously on all radiometers, only slight changes in the drain currents were observed w.r.t. the values measured on the single radiometers: this confirmed that the models used to group radiometers and to ordinate bias quadruplets in time was correct. Hence, no 1st order effects due to bias cross talk are expected to affect the radiometers performance.

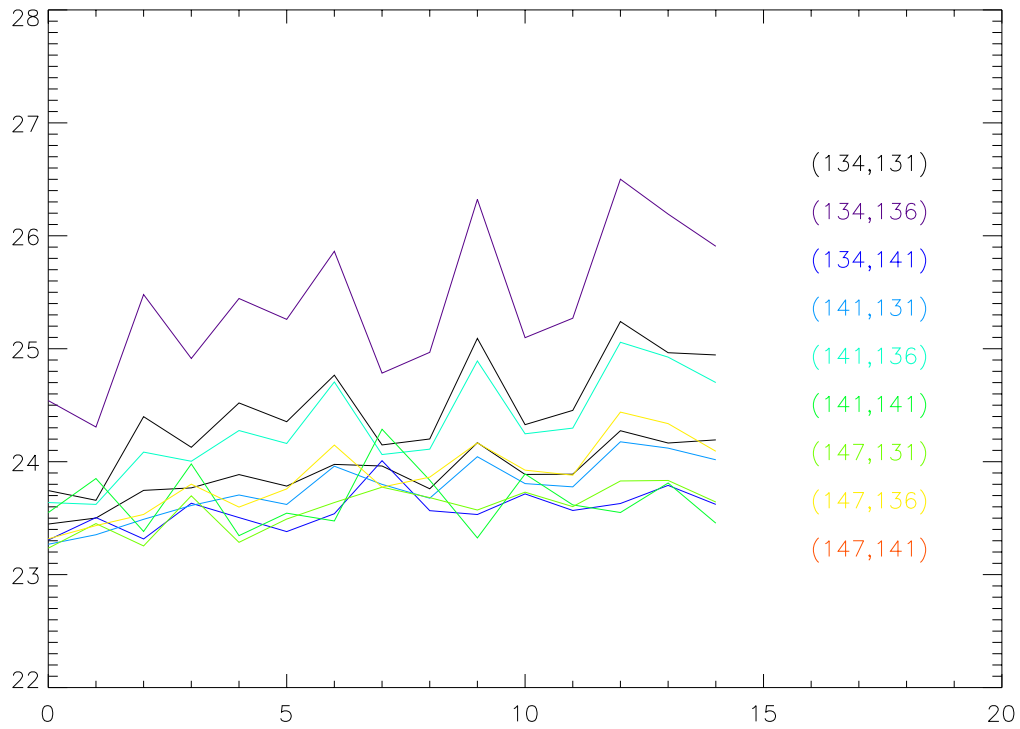


Here follows, for each of the channels, the bias changes adopted w.r.t. the automatic choice indicated by the code displaying tuning maps. Changes were made to seek for better balancing and to improve isolation, sometimes paying a few hundreds mK in terms on Noise Temperature.

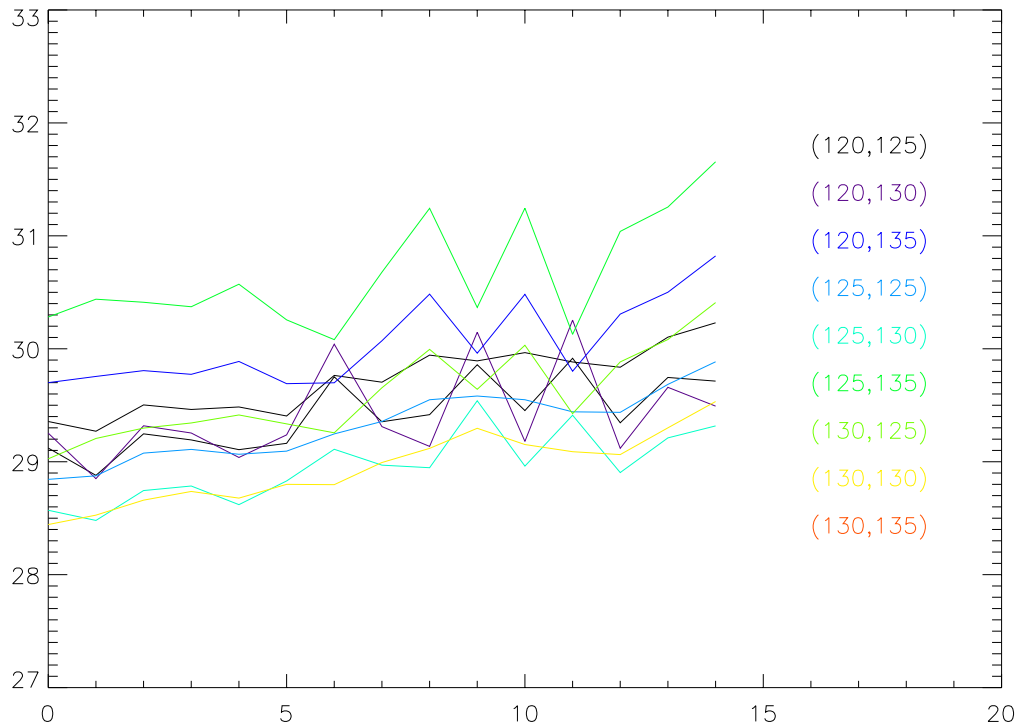
CH	VG	BEST BIAS Vg		Tn	Vd	new Vd
		M(0) /S(2)	M(1)/S(3)	(R0) /(R1)		
18 M	N	Vg1,Vg2	Vg1,Vg2	//	N	
18 S	Y	162,209	217,187	26.1, 28.7	N	
19M	Y	212,220	207,213	26.3, 25.8	N	
19 S	Y	207,222	210,228	28.6, 30.4	N	
20 M	N			//	N	
20 S	Y	188,231	172,226	32.3, 32.3	N	
21 M	Y	192,240	194,232	23.5, 24.9	Y	147,136
21 S	Y	190,215	217,235	28.7, 30.4	N	
22 M	Y	218, 210	188,188	27.5, 28.1	Y	130,135
22 S	Y	210,221	199,222	27.3, 29.2	N	
23 M	Y	201, 206	192,223	29.8, 28.7	N	
23 S	Y	184, 213	198,213	31, 29.9	Y	
24 M	Y	232, 205	227,204	21.7, 21.3	N	
24 S	Y	217, 207	225,206	21.5, 22.4	N	
25 M	Y	215, 200	218,200	23.6, 23.1	Y	177,178
25 S	Y	223, 195	223,199	21, 20.9	N	
26 M	Y	226, 205	221,197	24.6, 27.1	N	
26 S	Y	222,196	234,198	20.3, 21.9	N	
27 M	Y	242, 97	244,108	17.4, 17.7	N	
27S	Y	237, 83	253,69	19.9, 17.9	N	
28 M	Y	240,101	237,156	16.7,17	Y	150,163
28 S	N	240,89	251,98	16.8,15.7	N	

Table 10 Summary of the changes applied w.r.t the best bias point automatically determined by the code. From left: channel, Vg bias change w.r.t. the best bias point (Y/N) , best bias quadruplet, Noise Temperature corresponding to the best bias quadruplet, Vd bias change (Y/N) , new Vd pair applied.

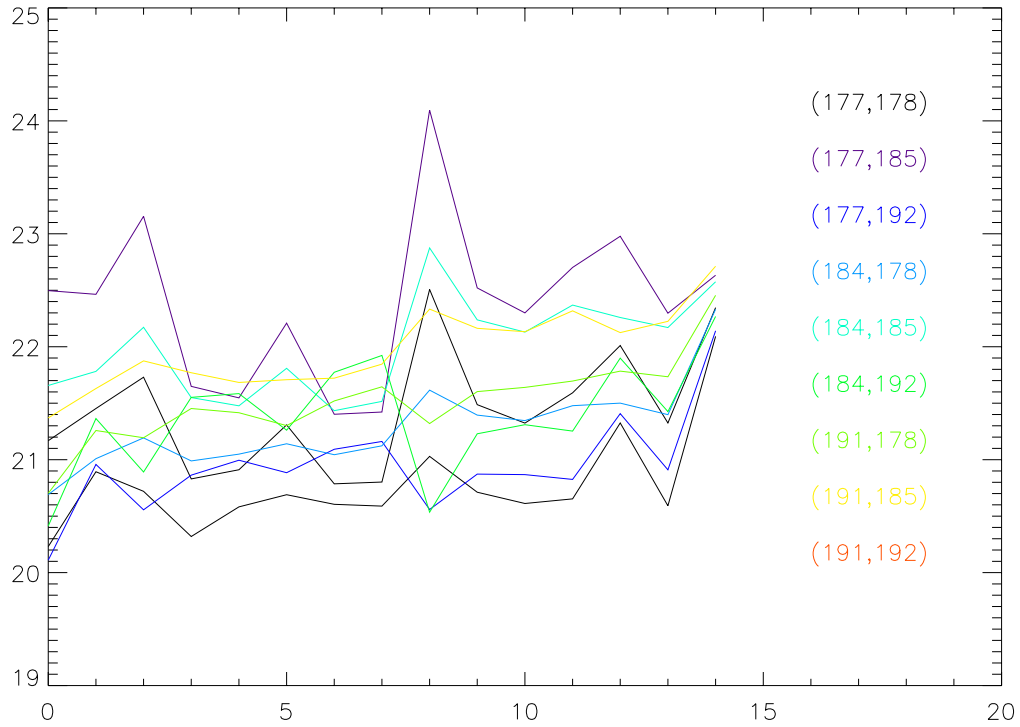
The Vd curves are displayed below for the four relevant cases reported in the table. On X axis is a sequential number characterizing the Vg bias quadruplet; on Y axis is reported the Noise Temperature. Each curve corresponds to a Vd bias pair. The Vd change was considered acceptable only in the case that the quadruplet considered the best Vg bias point from Vg maps analysis was contained in the Vd curves. Only in one case (LFI 28 M) the opposite criterion was followed (staring from Vd curves and looking for the same point in the Vg maps) , in order to find a trade off between Noise temperature, balancing , Isolation .



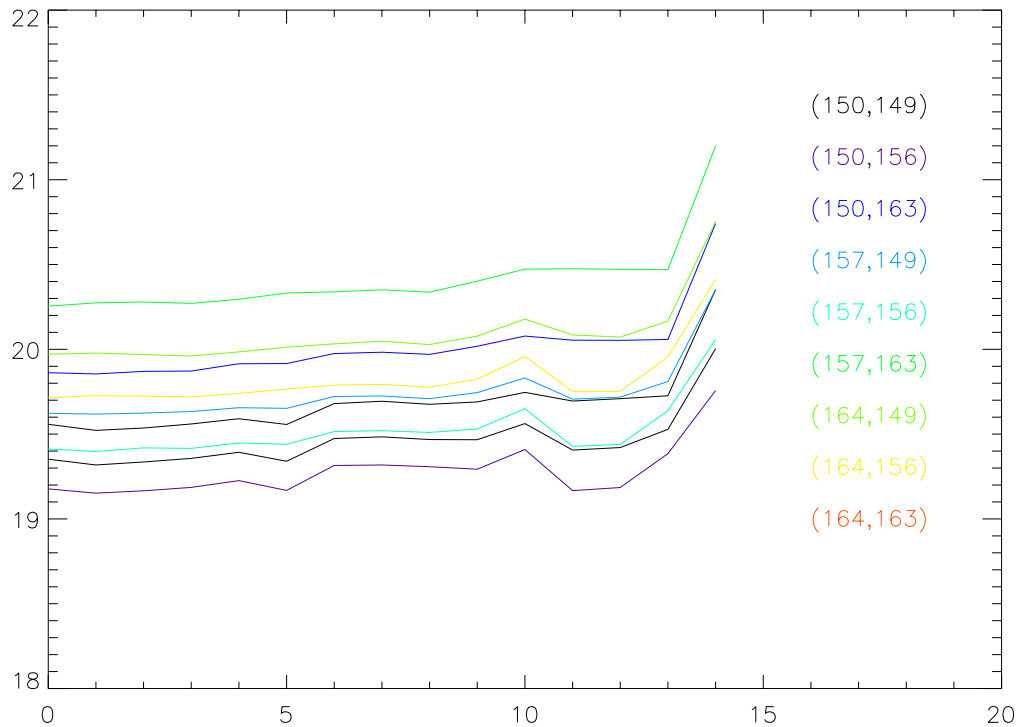
Plot 3 LFI 21-M



Plot 4 LFI 22-M



Plot 5 LFI 25-M



Plot 6 LFI 28- M



				vg1		vg2		vd		
CH27	00	00	M1	LP001320	242	F2	97	61	156	9C
CH27	01	01	M2	LP002320	255	FF	96	60	157	9D
CH27	02	10	S1	LP003320	235	EB	86	56	157	9D
CH27	03	11	S2	LP004320	248	F8	113	71	156	9C
CH24	04	00	M2	LP005320	227	E3	204	CC	183	B7
CH24	05	01	M1	LP006320	219	DB	204	CC	183	B7
CH24	06	10	S2	LP007320	225	E1	208	D0	152	98
CH24	07	11	S1	LP008320	218	DA	207	CF	157	9D
CH21	08	00	S2	LP009320	205	CD	243	F3	132	84
CH21	09	01	S1	LP010320	170	AA	221	DD	136	88
CH21	0A	10	M1	LP011320	192	C0	231	E7	147	93
CH21	0B	11	M2	LP012320	191	BF	224	E0	136	88
CH22	0C	00	S2	LP013320	193	C1	231	E7	130	82
CH22	0D	01	S1	LP014320	210	D2	221	DD	128	80
CH22	0E	10	M1	LP015320	208	D0	218	DA	130	82
CH22	0F	11	M2	LP016320	188	BC	188	BC	135	87
CH23	10	00	S2	LP017320	198	C6	213	D5	127	7F
CH23	11	01	S1	LP018320	180	B4	222	DE	123	7B
CH23	12	10	M1	LP019320	211	D3	206	CE	120	78
CH23	13	11	M2	LP020320	190	BE	228	E4	119	77
CH25	14	00	M1	LP021320	231	E7	203	CB	177	B1
CH25	15	01	M2	LP022320	218	DA	200	C8	178	B2
CH25	16	10	S1	LP023320	231	E7	196	C4	167	A7
CH25	17	11	S2	LP024320	223	DF	199	C7	166	A6
CH28	18	00	M1	LP025320	243	F3	101	65	150	96
CH28	19	01	M2	LP026320	240	F0	112	70	163	A3
CH28	1A	10	S1	LP027320	235	EB	81	51	157	9D
CH28	1B	11	S2	LP028320	249	F9	90	5A	158	9E
CH20	1C	00	S2	LP029320	169	A9	215	D7	127	7F
CH20	1D	01	S1	LP030320	179	B3	230	E6	132	84
CH20	1E	10	M1	LP031320	191	BF	244	F4	121	79
CH20	1F	11	M2	LP032320	209	D1	231	E7	127	7F
CH19	20	00	S2	LP033320	207	CF	222	DE	125	7D
CH19	21	01	S1	LP034320	202	CA	226	E2	120	78
CH19	22	10	M1	LP035320	205	CD	221	DD	124	7C
CH19	23	11	M2	LP036320	196	C4	216	D8	126	7E
CH18	24	00	S2	LP037320	216	D8	182	B6	114	72
CH18	25	01	S1	LP038320	155	9B	215	D7	138	8A
CH18	26	10	M1	LP039320	195	C3	189	BD	126	7E
CH18	27	11	M2	LP040320	198	C6	201	C9	125	7D
CH26	28	00	M2	LP041320	226	E2	200	C8	170	AA
CH26	29	01	M1	LP042320	247	F7	203	CB	169	A9
CH26	2A	10	S2	LP043320	240	F0	197	C5	169	A9
CH26	2B	11	S1	LP044320	227	E3	194	C2	172	AC

Table 11 Final bias table containing optimal tuned bias in the SCOS format.



4.6 CONCLUSIONS

Despite of the long duration and of the complicate procedure run, the Hyper Matrix Tuning was completed successfully. Actually, the HFI team was able to provide 4K reference load thermal conditions close to the requirement, enabling to perform the data analysis with a good accuracy.

Results revealed a very good internal consistency. In fact, all results obtained at the end of the fourth step were in good agreement with the Pre-Tuning analysis and with results from the CSL Tuning , at least for those bias points common to the two tests.

The non linear model , applied to the 30 and 44 GHz channels, provided optimal bias not far from the points chosen. Moreover, the analysis performed only on the fourth run using the pre-tuning method (to minimize the non linear behaviour of the radiometers) showed a good agreement with the linear model.

The tuning activity resulted in a new bias table where almost all the gate voltage bias have been changed w.r.t. the CSL values.

In several cases (four) the Drain voltage Tuning suggested that new drain voltage pairs could improve results.

For almost all the radiometers, tuning resulted in new bias configurations characterized by having , w.r.t. CSL setup:

- Lower noise temperature
- Improved Isolation
- Better LNAs drain current balancing



5 APPENDIX

Here follows the list of all the arguments described in the Appendix sections. They are annexed as separate documents in order to make it easier the reading of this document.

- 5.1 **Appendix 1 – 4K temperatures during the 4 Tuning runs**
- 5.2 **Appendix 2– Drain voltage tuning curves**
- 5.3 **Appendix 3 – comparison HYM Vs CSL results**
- 5.4 **Appendix 4 – 4th run MAPS with Pre-Tuning method**
- 5.5 **Appendix 5 – HYM- MAPS: linear analysis**
- 5.6 **Appendix 6 –HYM MAPS corrected for NON LINEARITY**
- 5.7 **Appendix 7-a –HYM MAPS corrected for non linearity and BEU thermal drift (cut 3 sigma)**
- 5.8 **Appendix 7-b –HYM MAPS corrected for non linearity and BEU thermal drift (cut 10 sigma)**